in $(\mu\text{-H})Os_3(CO)_{10}(\mu\text{-OCNHR})$, the M-M separation is found to be in the range 2.6-3.0 Å. In those cases, there should be an M-M bond according to the EAN rule. In complex **2a**, where the bridging iodine should be considered as a three-electron donor, no M-M bond is required in order to conform to the EAN rule. One could reasonably expect a longer M-M separation. The Os1-O7 and Os2-C7 distances are 2.056 (5) and 2.102 (7) Å, respectively. The Os-C(CO) distances are somewhat longer for two CO ligands trans to the terminal iodine ligand (1.92, 1.95 Å); the longest (1.98 Å), however, is observed for the CO trans to the carboxamido carbon atom. The carboxamido ligand shows partial double-bond character for both C=O (1.28 Å) and CN (1.34 Å) bonds, similar to many other complexes of the same type. For complex **4b**, pseudooctahedral geometry is again observed, exemplified by the cis interligand bond angle within the range 84.3 (2)-97.0 (4)° around the osmium metal. The three CO ligands are arranged in a facial configuration, with a somewhat longer Os-C distance for the CO trans to the amine ligand. The longer Os-N separation (2.197 (9) Å) than $Os-C_{av}$ (1.89 (1) Å) clearly indicates the π-acid character of the CO ligand. The Os-I separations, 2.735 (1) and 2.736 (1) Å, are normal bonding Os-I distances.

Acknowledgment. This work was supported by the National Science Council, Republic of China.

Registry No. **1a**, 113600-31-0; **1b**, 113600-36-5; **2a**, 113600-32-1; **4a**, 113600-34-3; **4b**, 113600-35-4; *trans*-**5**, 113600-33-2; *cis*-**5**, 113666-89-0; **6**, 17632-05-2; $(\mu\text{-Br})Os_2(CO)_6(\mu\text{-OCNHCHMe}_2)Br_2$, 113600-37-6; I_2, 7553-56-2; $OHCNHCHMe_2$, 16741-46-1; $OHCNHCMe_3$, 2425-74-3.

Supplementary Material Available: For the structure determinations of $(\mu\text{-I})Os_2(CO)_6(\mu\text{-OCNHCHMe}_2)I_2$ and $Os(CO)_3(NH_2CMe_3)I_2$, tables of anisotropic thermal parameters and complete interatomic distances and bond angles (4 pages); listings of calculated and observed structure factors (57 pages). Ordering information is given on any current masthead page.

Contribution from the Department of Chemistry,
City University of New York, Queens College, Flushing, New York 11367

Thermal and Photochemical Reactions of $Ru_3(CO)_{12}$ Adsorbed onto Porous Vycor Glass

Thomas Dieter and Harry D. Gafney*

Received October 15, 1987

$Ru_3(CO)_{12}$ physisorbs onto porous Vycor glass, PVG, without disruption or significant distortion of the complex. UV photolysis in vacuo and thermolysis at $T < 100$ °C lead to oxidative addition of a surface silanol group and quantitative formation of $(\mu\text{-H})Ru_3(CO)_{10}(\mu\text{-OSi}_{surf})$. The activation energies for formation of $(\mu\text{-H})Ru_3(CO)_{10}(\mu\text{-OSi}_{surf})$, 6.2 ± 0.4 kcal/mol, and regeneration of $Ru_3(CO)_{12}$ in the presence of CO, 5.1 ± 0.4 kcal/mol, suggest that these species are in dynamic equilibrium on the glass surface. The photoinduced oxidative addition is independent of excitation wavelength and occurs with a quantum yield of $(1.6 \pm 0.3) \times 10^{-2}$ with 350-nm excitation. The photochemistry of the adsorbed complex is interpreted within the current solution phase model where the specificity of the reaction arises not from chemical factors but from the rigidity and low dimensionality of the support.

Introduction

Interest in organometallic chemistry arises not only from the interdisciplinary nature of the chemistry, but the practical applications of these complexes in catalysis. Ruthenium complexes, for example, have been recognized as active catalysts of a number of transformations.[1-7] An alternative to homogeneous catalysis is to bind a potentially active reagent to a support, i.e., assemble a hybrid system.[8-10] $Ru_3(CO)_{12}$ physisorbs onto alumina and silica with the metal framework intact, and the adsorbed complex thermally decomposes to mononuclear species.[11] Basset and co-workers report that thermal activation of $Ru_3(CO)_{12}$ on silica gel leads to oxidative addition of a silanol group.[12] The grafted cluster, $HRu_3(CO)_{10}(OSi)$, decomposes at ≥100 °C to form aggragated metal particles covered with CO and a Ru(II) carbonyl species. On high surface area supports under H_2, thermal decomposition of $Ru_3(CO)_{12}$ at 350-400 °C yields small metal particles with a crystallite size of 15-20 Å that exhibit enhanced activity and selectivity in the hydrogenolysis of straight-chain hydrocarbon to methane.[13]

With few exceptions, the catalytic activity of Ru complexes, whether in homogeneous[1-7] or heterogeneous[8-18] systems, requires high temperatures and pressures. Consequently, there is an interest in the photochemical reactivity of these complexes. Photoactivation offers a route to catalytic intermediates under less stringent conditions and, since the thermal and photochemical reactions of $Ru_3(CO)_{12}$ differ,[19] the possibility of new reactive intermediates.

The photochemistry of $Ru_3(CO)_{12}$ in fluid solution has been interpreted in terms of cleavage of a Ru-Ru bond[20] and formation of an isomeric form of the ground state.[21] In a recent, extensive

(1) Strohmeier, W.; Weigelt, L. *J. Organomet. Chem.* **1978**, *145*, 189.
(2) Sanchez-Delgado, R. A.; deOchoa, O. L. *J. Mol. Catal.* **1979**, *6*, 303-5.
(3) Smith, A. K.; Basset, J. M. *J. Mol. Catal.* **1977**, *2*, 229-41.
(4) Castiglioni, M.; Milone, L.; Osella, D.; Vagilio, G. A.; Valle, M. *Inorg. Chem.* **1976**, *15*, 394-6.
(5) Knifton, J. F. *J. Mol. Catal.* **1980**, *11*, 91-105.
(6) King, R. B.; King, A. D.; Tanaka, K. *J. Mol. Catal.* **1981**, *10*, 75-83.
(7) Johnson, T. H.; Siegle, L. A.; Chaffin, J. K. *J. Mol. Catal.* **1980**, *9*, 307-11.
(8) Bailey, D. C.; Langer, S. H. *Chem. Rev.* **1981**, *81*, 109-48.
(9) Ichikawa, M. *CHEMTECH* **1982**, 674-80.
(10) Basset, J. M.; Choplin, A. J. *J. Mol. Catal.* **1983**, *21*, 95-108.
(11) Kuznetsov, V. L.; Bell, A. T.; Yermakov, Y. I. *J. Catal.* **1980**, *65*, 374-9.
(12) Theolier, A.; Choplin, A.; D'Ornelas, L.; Basset, J. M.; Zanderighi, G.; Sourisseau, C. *Polyhedron* **1983**, *2*, 119.
(13) Simpson, A. F.; Whyman, R. *J. Organomet. Chem.* **1981**, *213*, 157.
(14) Smith, A. K.; Theolier, A.; Basset, J. M.; Ugo, R.; Commereuc, D.; Chauvin, Y. *J. Am. Chem. Soc.* **1978**, *100*, 2590-1.
(15) Verdonck, J. J.; Jacobs, P. A.; Uytterhoven, J. B. *J. Chem. Soc., Chem. Commun.* **1979**, 181.
(16) Goodwin, J. G.; Naccache, C. *J. Mol. Catal.* **1982**, *14*, 259.
(17) Sanchez-Delgado, R. A.; Duran, I.; Monfort, J.; Rodriguez, E. *J. Mol. Catal.* **1981**, *11*, 193-203.
(18) Zecchina, A.; Guglielminotti, E.; Bossi, A.; Camia, M. *J. Catal.* **1982**, *74*, 225, 240, 266.
(19) Johnson, B. F. G.; Lewis, J.; Twigg, M. V. *J. Chem. Soc., Dalton Trans.* **1975**, 876; *J. Organomet. Chem.* **1974**, *67*, C75-6.
(20) Wrighton, M. S. *Ann. N.Y. Acad. Sci.* **1980**, Vol *333*, 188-207.
(21) Malito, J.; Markiewicz, S.; Poe, A. *Inorg. Chem.* **1982**, *21*, 4335-7.

0020-1669/88/1327-1730$01.50/0

study, Ford and co-workers report that population of the low-energy excited state leads to the formation of an isomeric form of the ground state that possesses a coordinatively unsaturated Ru center.[22,23] The latter, which is trapped by a two-electron donor, L, yields $Ru_3(CO)_{12}L$, which is the precursor to the fragmentation products.[22] A wavelength-dependent photosubstitution pathway occurs principally from higher energy excited states via CO dissociation to form the unsaturated $Ru_3(CO)_{11}$.[22] While this offers a detailed picture of the solution photochemistry, little information is currently available on the photoactivation of surface-confined $Ru_3(CO)_{12}$. Doi and Yano report that $Ru_3(CO)_{12}$ adsorbed onto silica exhibits a new absorption at 330 nm, and UV photolysis of the adsorbed complex leads to a monomeric species, which they postulate to be $Ru(CO)_4/SiO_2$.[24] Wrighton and Liu find that the photoinduced fragmentation of $Ru_3(CO)_9L_3$, where L denotes coordination to functionalized silica gel, is reversible.[25] Clearly, the chemical nature of the support surface influences reactivity.[11,12,17] In addition, although less well understood at present, Pfiefer and Avnir propose that geometric factors,[26] i.e., the dimensionality of the surface,[27-29] also affects reactivity. Amorphous materials, in particular, lack the geometric regularity that produces an equivalence of surface sites. The surface per se may impose constraints that lead to reaction pathways not found in fluid solution. Turro reports that the unprecedented photochemical reactions of dibenzyl ketone and its derivatives on zeolites, for example, are consistent with expectations based on the topological structure of the zeolite and the photochemical mechanism in homogeneous solution.[30]

The principal difficulty in quantitating the photochemical behavior of an adsorbed complex is the opacity of the support.[31] To circumvent this difficulty, we make use of Corning's Code 7930 porous Vycor glass, PVG. PVG is a transparent, surface-hydroxylated glass with a random array of interconnected 70 ± 21 Å diameter cavities. The similarities and differences between PVG and silica gel have been described.[32-34] In this paper, we describe the thermal and photochemical reactions of $Ru_3(CO)_{12}$ physisorbed onto this glass. The photochemistry of the adsorbed trimer is compared with that in deaerated, hydrocarbon solution, where both fragmentation and, in the presence of triphenylphosphine, monosubstitution of the trimer occurs.

Experimental Section

Materials. $Ru_3(CO)_{12}$ was obtained from Pressure Chemical Co. and used without further purification since its UV–visible and IR spectra were identical with published spectra.[22,35-40] $Ru(CO)_5$ and $Ru_3(CO)_9(PPh_3)_3$ were prepared according to literature procedures.[19,37,41] The UV spectrum of the pentacarbonyl and the electronic and IR spectra of $Ru_3(CO)_9(PPh_3)_3$ agreed with published spectra.[40,41] Triphenylphosphine, PPh_3 (Pfaltz & Bauer), was purified by recrystallization from ethanol. Tri-*tert*-butylphosphine, $P(t\text{-}Bu)_3$ (Alfa Ventron), 1,2-diphenylacetylene, DPA (Aldrich), and CO (Linde) were used as received since their reported purity is >99%. Spectral grade solvents were used as received, whereas reagent grade solvents were dried over CaH_2 and distilled prior to use. Freshly distilled 1-pentene (J. T. Baker) was passed through chromatographic grade alumina (J. T. Baker, Lot No. 33154) prior to use.

Code 7930 porous Vycor glass was obtained from the Corning Glass Works and used as either a powder (354–250 μm diameter particles) or 25 mm × 8 mm × 1 mm flat plates. The powdered and plate samples of PVG were extracted with distilled water for 24 h, dried under reduced pressure ($p \leq 10^{-4}$ Torr) at 60 °C, and then calcined in air at 500 °C for ≥24 h.[42-44] The calcined samples were stored at 500 °C. When needed, a sample was cooled to room temperature, 22 ± 1 °C, under vacuum and then impregnated by sublimation or solution adsorption procedures.[45,46]

Impregnation Procedures. Calcined powdered or plate samples of PVG were suspended over the solid complex in an evacuated flask. The flask was maintained at 50 °C for various times, and the amount of moles adsorbed was determined spectrally by comparison with samples prepared by solution impregnation. In the latter procedure, calcined, plate, or powdered PVG was placed in 50 mL of a 10^{-4} M *n*-pentane or isooctane solution of the trimer. Lowering the temperature of the isooctane solution to ≤10 °C markedly increased the amount of complex adsorbed. The amount of moles of $Ru_3(CO)_{12}$ adsorbed was calculated from the change in absorbance of the solution phase at 395 nm, and the solvent incorporated during impregnation was removed under vacuum or flowing N_2 at room temperature.[47,48] With lower loadings, however, the molar extinction coefficient of $Ru_3(CO)_{12}$ at 395 nm, $\epsilon = 7.7 \times 10^3$ M^{-1} cm^{-1},[38] was not large enough to accurately measure the moles of trimer adsorbed. Attempts to determine the amount adsorbed by monitoring the intense, 238-nm, MLCT band of the complex also proved to be unreliable due to the desorption of trace amounts of water. The latter resulted in a variable optical density at ≤250 nm that masked the small changes in optical density due to adsorption of the trimer. Consequently, in dilute samples, i.e., $\leq 10^{-8}$ mol of complex/g of PVG, the moles adsorbed were calculated from the ratio of the absorbance of the dried sample relative to that of a more concentrated, dried sample containing a known number of moles of Ru_3CO_{12} per gram. The uncertainity in the transmittance of the glass and the cross-sectional distribution of the adsorbed complex, however, introduces a 20% uncertainty in the moles adsorbed determined by this comparative procedure.[43] All manipulations of the impregnated samples were under a N_2 atmosphere.

Photochemical Procedures. Isooctane solutions of $Ru_3(CO)_{12}$, contained in 10 mm × 10 mm quartz cells and degassed by three freeze–pump–thaw cycles, were irradiated in a Rayonet reactor (Southern New England Ultraviolet Corp.) equipped with 350-nm bulbs. The light intensity, determined by ferrioxalate actinometry,[49,50] was typically 10^{-6} einstein/(L s). Impregnated plates of PVG were rigidly mounted with a Teflon holder in previously described rectangular quartz or pyrex cells.[42-44,47,48] Unless otherwise specified, the cell and enclosed sample were evacuated, and all samples were irradiated in vacuo ($p \leq 10^{-4}$ Torr). The plate samples were irradiated with 254, 310, or 350-nm light in the Rayonet reactor. Quantum yield measurements, however, were limited to 350-nm excitation where competitive absorption by the glass (50% *T* at 295 nm vs air) is negligible. The excitation intensity incident on the sample surfaces at this wavelength, typically 2×10^{-9} einstein/(s cm^2), was determined with ferrioxolate solutions of known surface area contained in identical rectangular cells. The photoinduced reactions were limited to ≤20%, and the initial rates of reactant consumption and product formation were calculated according to the method of Wong and Allen.[51] The average intensity absorbed by $Ru_3(CO)_{12}$ was calculated from the average of the initial and final absorbance of the trimer at 350

(22) Desrosiers, M. F.; Wink, D. A.; Trautman, R.; Friedman, A. E.; Ford, P. C. *J. Am. Chem. Soc.* **1986**, *108*, 1917–27.
(23) Desrosiers, M. F.; Wink, D. A.; Ford, P. C. *Inorg. Chem.* **1985**, *24*, 2–3.
(24) Doi, Y.; Yano, K. *Inorg. Chim. Acta* **1976**, *76*, L71–3.
(25) Liu, D. K.; Wrighton, M. S. *J. Am. Chem. Soc.* **1982**, *104*, 898–901.
(26) Pfiefer, P.; Avnir, D. *J. Chem. Phys.* **1983**, *79*, 3558–65.
(27) Avnir, D.; Farin, D.; Pfiefer, P. *J. Chem. Phys.* **1983**, *79*, 3566–71.
(28) Avnir, D.; Farin, D.; Pfiefer, P. *Nature (London)* **1984**, *308*, 261–3.
(29) Mandelbrot, M. M. *The Fractal Geometry of Nature*; Freeman: San Francisco, CA, 1982.
(30) Turro, N. J. *Pure Appl. Chem.* **1986**, *58*, 1219–28.
(31) Jackson, R. L.; Trusheim, M. R. *J. Am. Chem. Soc.* **1982**, *104*, 6590–6.
(32) Iler, R. K. *The Chemistry of Silica*; Wiley-Interscience: New York, 1979; p 551.
(33) Hair, M. L.; Chapman, I. D. *J. Am. Ceram. Soc.* **1966**, *49*, 651; *Trans. Faraday Soc.* **1965**, *61*, 1507.
(34) Cant, N. W.; Little, L. H. *Can. J. Chem.* **1964**, *42*, 802–9; **1965**, *43*, 1252–4.
(35) Calderazzo, F.; L'Eplattenier, F. *Inorg. Chem.* **1967**, *6*, 1220–4.
(36) Bruce, M. I.; Stone, F. G. A. *Angew. Chem., Int. Ed. Engl.* **1968**, *7*, 427–32.
(37) Candlin, J. P.; Shortland, A. C. *J. Organomet. Chem.* **1969**, *16*, 289–99.
(38) Battiston, G. A.; Bor, G.; Dietler, U. K.; Kettle, S. F. A.; Rossetti, R.; Sbrignadello, G.; Stanghellini, P. L. *Inorg. Chem.* **1980**, *19*, 1961–73.
(39) Tyler, D. R.; Levenson, R. A.; Gray, H. B. *J. Am. Chem. Soc.* **1978**, *100*, 7888–93.
(40) Bruce, M. I.; Shaw, G.; Stone, F. G. A. *J. Chem. Soc., Dalton Trans.* **1972**, 2094.
(41) Poe, A.; Twigg, M. V. *J. Chem. Soc., Dalton Trans.* **1974**, 1860; *Inorg. Chem.* **1974**, *13*, 2982–5.
(42) Wolfgang, S.; Gafney, H. D. *J. Phys. Chem.* **1983**, *87*, 5395–5401.
(43) Kennelly, T.; Braun, M.; Gafney, H. D. *J. Am. Chem. Soc.* **1985**, *107*, 4431–40.
(44) Wei, S.; Wolfgang, S.; Strekas, T. C.; Gafney, H. D. *J. Phys. Chem.* **1985**, *89*, 974–8.
(45) Ciapetta, F. G.; Plank, C. J. *Catalysis*; Emmett, P. H., Ed.; Reinhold: New York, 1954; Vol 1, p 315.
(46) Innes, W. B. *Catalysis*; Emmett, P. H., Ed.; Reinhold: New York, 1954; Vol 1, p 245.
(47) Simon, R. C.; Morse, D. L.; Gafney, H. D. *Inorg. Chem.* **1983**, *22*, 573–4.
(48) Simon, R. C.; Morse, D. L.; Gafney, H. D. *Inorg. Chem.* **1985**, *24*, 2565–70.
(49) Parker, C. A. *Proc. R. Soc. London, A* **1953**, *220*, 104.
(50) Hatchard, C. G.; Parker, C. A. *Proc. R. Soc. London, A* **1956**, *235*, 518.
(51) Wong, P. K.; Allen, A. O. *J. Phys. Chem.* **1970**, *74*, 774.

nm. Due to differences in light scattering by the glass and differences in the optical pathlength (see below), we estimate the uncertainty in the measured values to be ca. 25%.[43]

Impregnated powdered samples diluted 30:1 with KBr were irradiated in the vacuum chamber of a Harrick's FTIR diffuse reflectance accessory with 254-nm light from a pen lamp (Analamp, Model 90-0001-01) or ≥350-nm light from a Plexiglas-filtered high-pressure Xe lamp (SA Instruments). In the latter experiments, the excitation intensity was typically 10^{-7} einstein/(s cm^2).

Physical Measurements. UV–visible spectra of the adsorbate, relative to blank PVG that had been treated in an identical manner, were recorded on a Cary 14 adapted to accommodate the rectangular cells or a Perkin-Elmer Lamda 320 spectrophotometer equipped with a thermostated cell holder. Gaseous photoproducts were collected with a Toepler pump and quantitated by previously described GC procedures.[47,48] The detector response, calibrated with known pressures of CO in the photolysis cell, was linear in the moles of gas. Infrared spectra of solutions or KBr disks were recorded on a Perkin-Elmer Model 1330 spectrometer calibrated with polystyrene. Diffuse reflectance FTIR, DRIFT, spectra of the complex adsorbed onto powdered PVG diluted with KBr (30:1) were recorded on a Nicolet 20DX FTIR equipped with an intensified IR source, an MCTB detector maintained at 77 K, and a Harrick's diffuse reflectance accessory. The interferograms were terminated under Happ–Ganzel apodization and converted to Kubelka–Munk spectra for quantitative comparison.[52] All spectra were ratioed against a background spectrum of blank, calcined PVG diluted 30:1 with KBr.

Results

Solution Photochemistry. Under 1 atm of CO, a 350-nm photolysis of $Ru_3(CO)_{12}$ in degassed isooctane causes a decline in absorbance at 238 and 394 nm, characteristic of the trimer.[39] A concurrent growth in absorbance at 260 nm establishes the formation of $Ru(CO)_5$.[39] The pentacarbonyl is unstable and, depending on the CO pressure, quantitatively reverts to the thermodynamically favored trimer. Infrared spectra recorded during 350-nm photolysis in the presence of 1-pentene show a decline in the trimer bands[24] at 2061 (vs), 2031 (s), and 2012 cm^{-1} (m) and the growth of new absorptions at 2100 (w), 2018 (s), and 1992 cm^{-1} (m), which are in excellent agreement with the reported spectrum of $Ru(CO)_4$(1-pentene).[53] At room temperature, 22 ± 1 °C, the 1-pentene adduct is unstable and quantitatively reverts to the trimer within minutes after photolysis. A 350-nm photolysis in the presence of diphenylacetylene, DPA, causes a decline in the 395-nm absorption. IR spectra show a decline in the $Ru_3(CO)_{12}$ bands and the appearance of bands at 2111 (w), 2082 (w), 2039 (ms), 2031 (m), and 2002 cm^{-1} (m), which are tentatively assigned to $Ru(CO)_4$(DPA).

In the presence of PPh_3, 350-nm photolysis of $Ru_3(CO)_{12}$ leads to a more complex reaction sequence. The solution changes from light yellow to transparent and ultimately to pink. A decline in the 395-nm absorption of $Ru_3(CO)_{12}$,[39] which corresponds to the initial color change, is accompanied by the growth of IR bands at 2061 (m), 1988 (w), and 1955 cm^{-1} (s), which confirms the formation of $Ru(CO)_4(PPh_3)$.[19] Continued photolysis gives rise to a light pink solution and the precipitation of red, needle-like crystals. Electronic and IR spectra of the precipitate are equivalent to the reported spectra of $Ru_3(CO)_9(PPh_3)_3$.[41] During precipitation of $Ru_3(CO)_9(PPh_3)_3$, the bands characteristic of the dodecacarbonyl continue to decline. The intensity of the 1955-cm^{-1} band of $Ru(CO)_4(PPh_3)$ also declines and a new absorption at 1909 cm^{-1}, which corresponds to the reported spectrum of the disubstituted, monomeric complex $Ru(CO)_3(PPh_3)_2$[53] becomes the dominant spectral feature (see paragraph at end of paper regarding supplementary material). In addition, spectral subtraction reveals weak bands at 2098, 2047, 2014, 1986, and 1974 cm^{-1}, which agree with the reported spectrum of $Ru_3(CO)_{11}(PPh_3)$.[40] The intensities of the latter bands remain essentially constant until all of the dodecacarbonyl reacts. Although this suggests that $Ru_3(CO)_{11}(PPh_3)$ is in a steady-state concentration, the spectral changes are not sufficiently resolved to determine whether the subsequent reactions of $Ru_3(CO)_{11}(PPh_3)$ lead to monomeric products or the trisubstituted trimer.

Different behavior occurs in the presence of tri-*tert*-butylphosphine, P(*t*-Bu)$_3$. A 350-nm photolysis causes a decline in the 395-nm band of $Ru_3(CO)_{12}$ and the appearance of IR bands at 2059, 1983, and 1945 cm^{-1}. The latter are assigned to $Ru(CO)_4(P(t\text{-}Bu)_3)$ because of their close similarity to the reported spectrum of $Ru(CO)_4(PPh_3)$.[19] However, bands attributable to the monosubstituted trimer, $Ru_3(CO)_{11}(P(t\text{-}Bu)_3)$, or the disubstituted monomer, $Ru(CO)_3(P(t\text{-}Bu)_3)_2$, assuming that their spectra would also resemble those of the PPh_3 analogue,[19,54] are not detected.

Table I. Limiting Quantum Yields of $Ru_3(CO)_{12}$ Fragmentation in Hydrocarbon Solution

ligand	$10^2\phi_{lim}$	ligand	$10^2\phi_{lim}$
1-pentene	8.0 ± 0.7[a]	P(*t*-Bu)$_3$	8.4 ± 0.5[b]
PPh_3	5.7 ± 0.4[b]	CO	10.5 ± 2.2[d]
PPh_3	4.4 ± 0.4[c]		

[a] Degassed isooctane, 22 ± 1 °C, 350-nm excitation. [b] Degassed *n*-pentane, 22 ± 1 °C, 350-nm excitation. [c] Reference 22. [d] Reference 21.

For comparison with the photochemistry on PVG, $Ru_3(CO)_{12}$ fragmentation quantum yields were measured in degassed *n*-pentane and isooctane with 350-nm excitation. At this wavelength, absorption by the glass is negligible. The observed yields, ϕ_{obsd}, were corrected for thermal reversibility, which occurs to some extent with each scavenging ligand, by extrapolating the time-dependent absorbance change after photolysis back to the end of photolysis. Plots of $1/\phi_{obsd}$ vs $1/[L]$ (see paragraph at end of paper regarding supplementary material), where L = 1-pentene, PPh_3, and tri-*tert*-butylphosphine (P(*t*-Bu)$_3$), are linear and the extrapolated values of ϕ_{lim} are listed in Table I. With P(*t*-Bu)$_3$ and 1-pentene as scavengers, the values of ϕ_{lim} are identical and within experimental error of the limiting yield, $(10.5 \pm 2.2) \times 10^{-2}$, reported by Poe and co-workers with CO as the scavenging ligand.[21] The limiting yield obtained with PPh_3, $(5.7 \pm 0.4) \times 10^{-2}$, is slightly smaller but similar to the essentially wavelength-independent value (405–313 nm) reported by Ford and co-workers.[22] In cyclohexane with 0.001–0.1 M PPh_3, linear plots of the reciprocal of the fragmentation quantum yield vs the reciprocal of the PPh_3 concentration gave 0.040 ± 0.004 as the limiting fragmentation yield.[22] For the purpose of comparison, the fragmentation quantum yield, $(7.4 \pm 3.0) \times 10^{-2}$, is taken as a lower limit of the quantum yield of formation of the precursor to fragmentation. In addition to fragmentation, spectral subtraction reveals a concurrent formation of $Ru_3(CO)_{11}(PPh_3)$. The relative band intensities suggest that formation of the monosubstituted trimer accounts for ≤10% of the observed reactivity during 350-nm photolysis. Relative to the limiting yield of fragmentation in the presence of PPh_3, 0.057 ± 0.04, this places the quantum yield of $Ru_3(CO)_{11}(PPh_3)$ at $\leq 6 \times 10^{-3}$ under our conditions.

Spectral Properties of $Ru_3(CO)_{12}$(ads). Whether impregnation is by sublimation or adsorption from solution, it occurs without change in the spectrum of the adsorbate or adsorbent. DRIFT spectra of calcined PVG (see paragraph at end of paper regarding supplementary material) indicate a surface composed of individual silanol groups, 3750 cm^{-1}, and associated, i.e., hydrogen-bonded, silanol groups.[33,34] Hair and Little and their co-workers report that the latter appears as a resolved band at 3660 cm^{-1}.[33,34] The band is not resolved in our experiments but is present as a distinct shoulder at 3655 cm^{-1} on the intense, 3750 cm^{-1}, individual silanol vibration. Other than a decrease in relative intensity, adsorption of $\leq 10^{-5}$ mol of $Ru_3(CO)_{12}$/g does not affect the silanol bands.

UV–visible spectra of $Ru_3(CO)_{12}$(ads) recorded at different locations on an impregnated sample are within experimental error, which establishes a uniform distribution of the complex on the

(52) *Nicolet Operations Manual*; Nicolet Analytical Instruments: Madison, WI, 1985.

(53) Austin, R. G.; Paonena, R. I.; Giordano, P. J.; Wrighton, M. S. *Adv. Chem. Ser.* **1978**, *No. 168*, 189–213.

(54) Johnson, B. F. G.; Johnson, R. D.; Josty, P. L.; Lewis, J.; Williams, I. G. *Nature (London)* **1967**, *213*, 901–2.

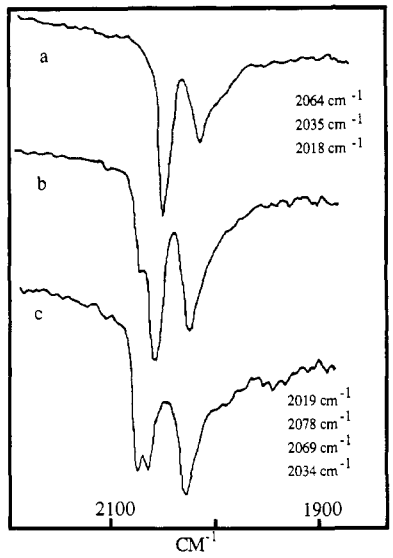

Figure 1. Diffuse reflectance FTIR spectra of (a) $Ru_3(CO)_{12}$(ads), (b) $Ru_3(CO)_{12}$(ads) during 350-nm photolysis in vacuo, and (c) (μ-H)$Ru_3(CO)_{10}$(μ-OSi_{surf}).

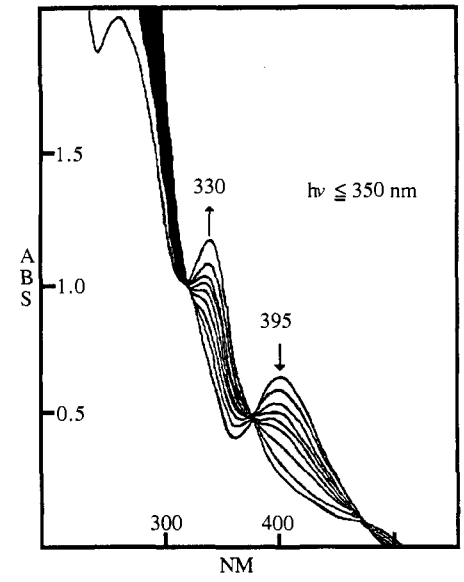

Figure 2. Electronic spectra recorded during 350-nm photolysis in vacuo of a sample containing 2×10^{-7} mol of $Ru_3(CO)_{12}$(ads)/g of PVG.

PVG surface.[42,43,48] As found with other metal carbonyls, however, the cross-sectional distribution is not uniform.[48,55] Regardless of the moles of $Ru_3(CO)_{12}$ adsorbed onto the plate samples, which ranged from 10^{-8} to 10^{-6} mol/g of PVG in these experiments, the complex uniformly impregnates volumes adjacent to the outer geometric surfaces of the sample. Impregnation of the interior cavities can be achieved but requires exposures to the impregnating solution considerably longer than the ≤12 h used in these experiments. Since the rate of desorption from the powder exceeds that from plate PVG, we assume that adsorption is also limited to the outer surfaces, where the larger amount adsorbed, 10^{-5} mol/g, is attributed to the larger external surface area of the glass powder.[55] In a porous support in which the adsorbate is not uniformly distributed, surface coverage can not be rigorously defined. Assuming the surface area within the impregnated regions is 130 m^2/g,[43] however, the maximum surface coverage in both the plate and powdered samples is estimated to be ≤1%.

Regardless of method, impregnation occurs without decomposition of $Ru_3(CO)_{12}$. GC analysis of the surrounding vapor phase after the complex is sublimed onto PVG gives no indication of CO, CO_2, or H_2 evolution, and the adsorbed trimer retains the spectral characteristics found in fluid solution. In the 230–500-nm region, the UV–visible spectrum of $Ru_3(CO)_{12}$(ads) is within experimental error in band maximum, band half-width, and relative extinction coefficient of the spectrum of the complex in isooctane. Spectral agreement, particularly in the UV region, occurs provided that PVG is rigorously dehydrated prior to impregnation. Trace amounts of chemisorbed water result in a variable absorbance in unimpregnated PVG at ≤250 nm. Consequently, the ratio of $Ru_3(CO)_{12}$(ads) absorbance at 238 nm relative to that at 395 nm varies considerably from sample to sample, and differs from the value that occurs in isooctane solution, 5.0 ± 0.1. On removal of the water, however, the ratio is constant from sample to sample, and within experimental error of that in isooctane.

The DRIFT spectrum of the adsorbed trimer (Figure 1) consists of bands at 2064 (s), 2035 (m), and 2018 cm^{-1} (sh) that, although shifted 2–6 cm^{-1} to higher wavenumbers, retain the relative intensity pattern found in fluid solution. Broadening of the lower frequency bands occurs, but a correlation splitting of the high-frequency band, characteristic of polycrystalline $Ru_3(CO)_{12}$,[56] is not present.

Photochemical Reactions of $Ru_3(CO)_{12}$(ads). A 350-, 310-, or 254-nm photolysis of $Ru_3(CO)_{12}$(ads) in vacuo causes the spectral changes illustrated in Figure 2. A decline at 395 nm and in the UV region is accompanied by a concurrent increase at 330 nm. Isosbestic points at 290 and 365 nm are maintained through 80% reaction, and the spectral changes are independent of the amount of $Ru_3(CO)_{12}$(ads), although, as mentioned above, the maximum loading is 10^{-6} mol/g. GC analysis of the vapor phase indicates the evolution of 1.8 ± 0.3 mol of CO/mol of $Ru_3(CO)_{12}$(ads) reacted; the latter is determined from the decline in absorbance at 395 nm. H_2 evolution, indicative of metal oxidation,[57] or CO_2 evolution is not detected, and exposing the photoproduct to 1 atm of CO regenerates $Ru_3(CO)_{12}$(ads) in ≥90% yield. IR spectra show a decline in the bands characteristic of the trimer and the appearance of a weak band at 2109 cm^{-1}, two relatively intense bands at 2078 and 2069 cm^{-1}, and a broad band at 2034 cm^{-1} with shoulders at 2017 and 1999 cm^{-1} (Figure 1). Bands in the bridging CO region indicative of dimeric complexes or bands indicative of monomeric complexes are not detected, and there is no evidence in the electronic spectra of trimer substitution.

The photoproduct ν_{CO} band pattern is characteristic of trimeric oxidative addition products. Complexes of the general formula $HRu_3(CO)_{10}L$, where L is OSi, SC_2H_5, and NO, for example, exhibit a similar band pattern; a medium- or low-intensity band above 2100 cm^{-1}, two strong bands in the 2080–2055-cm^{-1} region, and a broad, medium-intensity band in the 2030-cm^{-1} region with low-frequency shoulders.[12,58,59] Although shifted to higher frequency, oxidative addition products of the analogous Os trimer exhibit a similar spectral pattern.[58-60] Thermal activation of $Ru_3(CO)_{12}$ physisorbed onto silica gel, a hydroxylated surface similar to that of PVG,[33,34] leads to an oxidative addition of a surface silanol group.[12] This species, designated $HRu_3(CO)_{10}$(OSi_{surf}), exhibits an electronic absorption at 330 nm, and IR bands at 2111 (w), 2077 (s), 2066 (s), 2033 (br), and 1995 cm^{-1}.[12] The stoichiometry of the photoreaction and the spectral similarity with known oxidative-addition products establish the photoreaction on PVG to be

$$Ru_3(CO)_{12}(ads) \rightarrow HRu_3(CO)_{10}(OSi_{surf}) + 2CO \quad (1)$$

where $HRu_3(CO)_{10}(OSi_{surf})$ represents oxidative addition of a surface silanol group.

The extent of reaction 1 exhibits a dependence on unexpected parameters such as the volume of the photolysis cell and the

(55) Darsillo, M. S.; Paquette, M. S.; Gafney, H. D. *J. Am. Chem. Soc.* **1987**, *109*, 3275–86.
(56) Kettle, S. F. A.; Stanghellini, P. L. *Inorg. Chem.* **1979**, *18*, 2759–54.
(57) Yermakov, Y. I. *J. Mol. Catal.* **1983**, *21*, 35–54.
(58) Crooks, G. R.; Johnson, B. F. G.; Lewis, J.; Williams, I. G. *J. Chem. Soc. A* **1969**, 797–9.
(59) Johnson, B. F. G.; Raithby, P. R.; Zuccaro, C. J. *J. Chem. Soc., Dalton Trans.* **1980**, 99.
(60) Besson, B.; Moraweck, B.; Smith, A. K.; Basset, J. M. *J. Chem. Soc., Chem. Commun.* **1980**, 569–71.

Table II. Rate Constants and Activation Energies for (A) Thermal Formation of $(\mu\text{-H})Ru_3(CO)_{10}(\mu\text{-OSi}_{surf})$ and (B) Its Thermal Reaction with CO

(A) $Ru_3(CO)_{12}(ads) \rightarrow (\mu\text{-H})Ru_3(CO)_{10}(\mu\text{-OSi}_{surf})$

temp, °C	$10^{-4}k$, s^{-1}	E_a, kcal/mol
30.0	2.32 ± 0.06	6.2 ± 0.4
38.0	3.23 ± 0.04	
47.5	4.63 ± 0.07	

(B) $(\mu\text{-H})Ru_3(CO)_{10}(\mu\text{-OSi}_{surf}) + 2CO \rightarrow Ru_3(CO)_{12}(ads)$

temp, °C	P_{CO}, Torr	$10^{-5}k$, s^{-1}	E_a kcal/mol
42.0	160	2.43 ± 0.04	5.1 ± 0.4
51.0	160	2.96 ± 0.06	
64.5	160	3.39 ± 0.04	
69.0	160	5.28 ± 0.05	

presence of gases such as N_2 and He, although spectra recorded during photolysis confirm that neither gas is formally involved in the reaction. Provided the photodissociated CO is continuously removed, the photoreaction is quantitative. A complete loss of absorbance at 395 nm occurs with isosbestic points at 365 and 290 nm, and exposure to CO (1 atm) regenerates $Ru_3(CO)_{12}(ads)$ in ≥90% yield. With continuous removal of the evolved CO, the quantum yield of reaction 1 with 350 nm excitation is $(3.0 \pm 0.4) \times 10^{-2}$. Competitive absorption by PVG precludes quantum yield measurements with higher energy excitation. However, the similarity of the spectral changes during 254- or 310-nm photolyses with those during 350-nm photolysis (Figures 1 and 2) indicates that reaction 1 is independent of the excitation wavelength.

In a closed cell, the reaction proceeds to a photostationary state where the extent of conversion depends on the photolysis cell volume and/or the pressure of an inert gas. As cell volume increases, the extent of reaction 1 increases, whereas increasing the pressure of He decreases the extent of reaction. Under 1 atm of CO, no reaction occurs, and the addition of CO (1 atm) during photolysis in vacuo immediately quenches formation of $HRu_3(CO)_{10}(OSi_{surf})$, which, on standing under CO, thermally reverts to $Ru_3(CO)_{12}(ads)$.

Reaction 1 also occurs thermally, and was examined as a function of temperature to gain some insight into the energetics of formation of the oxidative addition product. Samples containing ca. 10^{-6} mol of $Ru_3(CO)_{12}(ads)/g$ in vacuo were shielded from light and stored in a constant-temperature bath. First-order plots of the change in absorbance at 330 nm, characteristic of the oxidative addition product, vs time are linear, and the rate constants, measured at temperatures between 30 and 47.5 °C, are summarized in Table II. An Arrhenius plot of the data yields an activation energy of 6.2 ± 0.4 kcal/mol.

The stability of the oxidative addition product, which exists for days at room temperature in vacuo, most likely arises from the bonding to the glass. Yet, stability is not at the expense of subsequent thermal reactivity. $HRu_3(CO)_{10}(OSi_{surf})$ quantitatively reverts to $Ru_3(CO)_{12}(ads)$ under a CO atmosphere, and this reaction was also examined as a function of temperature to determine the relative energies of reactant and product. Samples containing ca. 10^{-6} mol of $Ru_3(CO)_{12}(ads)/g$ were photolyzed under continuous pumping to 30–40% conversion with 350-nm light. After thermal equilibration in a constant-temperature bath, the samples were exposed to 160 Torr of CO and stored in the dark. The reaction, monitored by the increase in absorbance at 395 nm, characteristic of $Ru_3(CO)_{12}(ads)$, follows pseudo-first-order kinetics, and the rate constants measured at various temperatures are summarized in Table II. An Arrhenius plot of the data yields an activation energy of 5.1 ± 0.2 kcal/mol. Reactivity is not limited to only CO. In fact, although the details of the reactions are not presently clear, exposing $HRu_3(CO)_{10}(OSi_{surf})$ at room temperature to ligands such as PPh_3, $P(t\text{-Bu})_3$, and 1-pentene causes immediate reaction.

The photochemical and thermal reactions of $Ru_3(CO)_{12}$ in isooctane and *n*-pentane solutions containing the O-donor ligand triphenylsilanol, ethanol, THF, or 1,4-dioxane, were examined as possible models of reaction 1. Although a reaction occurred in the presence of each ligand, none of the solution reactions, whether thermally or photochemically activated, exhibit the specificity found on PVG. However, a number of spectral similarities to the reaction on PVG did occur in the presence of ethanol. A 350-nm photolysis of deareated pentane solution 10^{-4} M in $Ru_3(CO)_{12}$ and 10^{-1} M in ethanol causes an immediate decline in absorbance at 395 nm. After complete loss of the 395-nm absorption, continued photolysis results in the appearance of the 330-nm absorbance. IR spectra of the photolyte exhibiting the 330-nm absorption confirm the loss of the $Ru_3(CO)_{12}$ bands and reveal product bands at 2125 (w, br), 2089 (w, br), and 1973 (vw, br) cm^{-1} that are qualitatively similar to those of $HRu_3(CO)_{10}(OSi_{surf})$. Adding $P(t\text{-Bu})_3$ to the photolyte results in the immediate loss of the 330-nm absorption and the appearance of a band at 470 nm, which agrees with the visible absorption of $Ru_3(CO)_9(P(t\text{-Bu})_3)_3$. In view of the time dependence of the electronic spectral changes, however, the product spectrum can not be definitively assigned to a single species. The reaction appears to consist of several steps with the quantum efficiency of $Ru_3(CO)_{12}$ disappearance being very low, $<10^{-4}$.

Discussion

Ford and co-workers offer strong evidence that fragmentation proceeds via an isomeric form of the complex that possesses a coordinatively unsaturated metal center.[22,23] This species is trapped by a two-electron donor to form the precursor to fragmentation. The quantum yield of fragmentation is essentially independent of excitation wavelength (313–405 nm), and the reaction is thought to arise from the lowest energy excited state, which is antibonding with respect to the metal–metal bonds of the cluster.[22] Photosubstitution originates from a higher energy excited state where CO dissociation yields the unsaturated or solvated intermediate, which is trapped to form the monosubstituted trimer.[22]

With PPh_3 and $P(OCH_3)_3$ as scavenging ligands, Ford and co-workers find that the inverse of the observed fragmentation quantum yield is a linear function of the inverse of the scavenger concentration (0.001–0.1 M) with intercepts that indicate limiting fragmentation quantum yields of 0.040 ± 0.004 and 0.044 ± 0.006, respectively, in cyclohexane.[22] Similar results occur in *n*-pentane and isooctane, although the concentration range examined in our experiments is significantly smaller. Plots of ϕ_{obsd}^{-1} vs. $[L]^{-1}$ (see paragraph at end of paper regarding supplementary material) extrapolate to limiting fragmentation yields that are in reasonable agreement, considering that the value is dependent on the solvent and the scavenging ligand, with previously reported values (Table I). These data suggest that the quantum yield of formation of the precursor to fragmentation is $(7.3 \pm 3.0) \times 10^{-2}$ in fluid solution.

Substitution of the trimer is detected in the presence of PPh_3. Spectral subtraction reveals bands that agree in both band maxima and relative intensity with the reported spectrum of $Ru_3(CO)_{11}(PPh_3)$.[40] Although the estimated quantum yield of this pathway, $\lesssim 6 \times 10^{-3}$ in isooctane with 350-nm excitation, is less than the values found for $P(OCH_3)_3$ substitution in octane and cyclohexane,[22] the 350-nm photochemistry of $Ru_3(CO)_{12}$ in deareated *n*-pentane and isooctane is consistent with the model proposed by Ford and co-workers.

Adsorption of $Ru_3(CO)_{12}$ onto PVG occurs without evolution of possible decomposition products,[55] or significant spectral change. The electronic spectrum of $Ru_3(CO)_{12}(ads)$ is within experimental error in relative extinction coefficient, band maxima, and band half-width of values computed from fluid solution spectra.[39] Although shifted 2–6 cm^{-1} to higher frequency, the ν_{CO} band pattern closely resembles the fluid solution spectrum.[24,35,37] The shift is attributed to a slight polarization of electron density in the CO ligand, principally that in the π^* orbital, due to the anionic character of the PVG surface.[61] Broadening of the lower energy

(61) Basu, A.; Clark, J.; Perettie, D. J.; Gafney, H. D. *J. Phys. Chem.* **1983**, *87*, 4538–4543.
(62) Johnson, B. F. G.; Lewis, J.; Pippard, D.; Raithby, P. R. *J. Chem. Soc., Chem. Commun.* **1978**, 551–2.

ν_{CO} modes occurs, but changes in the relative intensities of specific axial or equatorial CO modes that might be attributed to a preferential orientation of the trimer on the surface are not detected. The similarity with solution spectra[24,35,39] establishes that $Ru_3(CO)_{12}$ physisorbs onto PVG without disruption or significant distortion of the complex. The absence of correlation splittings of the CO bands[56] and optical spectra recorded at different locations on the same sample establish that the adsorbed trimer exists as individual molecular entities uniformly distributed on the PVG surface. Consequently, changes in the photoreactivity of the adsorbed trimer cannot be attributed to molecular changes caused by adsorption or aggregation on the surface.

In spite of the spectral agreement, the photochemistry of $Ru_3(CO)_{12}$(ads) differs from that found in fluid solution. The immediate difference is the absence of monomeric products when $Ru_3(CO)_{12}$(ads) is photolyzed in the presence of scavenging ligands. Optical and IR spectra recorded during prolonged 300- or 350-nm photolysis of $Ru_3(CO)_{12}$(ads) under 1 atm of CO or 0.25 atm of P(*t*-Bu)$_3$, for example, indicate that the quantum yield of formation of monomeric products is $\leq 10^{-5}$. PVG is a highly irregular, porous support. Nevertheless, the absence of monomeric products cannot be attributed to restricted access of the scavenger to the photoexcited adsorbate. As noted above, the majority of $Ru_3(CO)_{12}$(ads) is on the outer surfaces of the PVG sample, and the quenching of reaction 1 by CO establishes, at least with smaller molecules, that scavengers in the surrounding gas phase do have access to the photoexcited adsorbate. Scavenging of photogenerated transients on PVG has also been shown to occur in a number of reaction systems.[42,43,48,55] Nor is the absence of monomeric products due to product instability since $Ru(CO)_5$ prepared photochemically in solution and adsorbed onto PVG is stable.

The stoichiometric and spectral data obtained in these experiments indicate a quantitative, photoinduced oxidative addition of a surface silanol group. Oxidative addition to either an individual Ru atom or across a Ru–Ru bond results in a reduction of molecular symmetry from D_{3h} to C_{2v}. The weak band at 2109 cm^{-1} in the product spectrum (Figure 1c) is assigned to the symmetric A_1 mode since a comparable band occurs at 2117 cm^{-1} in the spectrum of polycrystalline $Ru_3(CO)_{12}$.[56] Although fully allowed, typically the intensity of the A_1 band remains low, but its appearance is consistent with an adsorbed photoproduct of C_{2v} molecular symmetry. Oxidative addition to an individual Ru atom, on the other hand, yields a terminal Ru–H bond that generally exhibits a more intense IR band than vibrations due to a bridged hydrogen.[63] Spectra recorded in these experiments, however, offer no indication of a terminal Ru–H vibration. Rather, the photoproduct spectra (Figures 1 and 2) are equivalent to a series of Ru and Os oxidative addition products, $HM_3(CO)_{10}L$ (L = SR, OH, NO, and OSi), where addition across the metal–metal bond has been established.[11,58–60] Thus, UV photolysis of $Ru_3(CO)_{12}$(ads) leads to oxidative addition of a surface silanol group across an Ru–Ru bond and quantitative formation of the surface grafted species

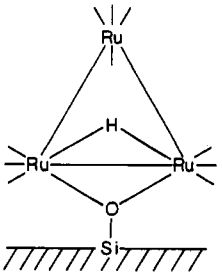

Oxygen, which anchors the complex to the support, acts as a three-electron donor and hydrogen binds to the metal cluster with a two-electron, three-center bond.[64] The stability of the grafted cluster, which exists for weeks in vacuo at room temperature, is due to the formation of the Ru–O bonds. Yet, stability is not at the expense of subsequent thermal reactivity. Exposing (μ-H)$Ru_3(CO)_{10}(\mu\text{-}OSi_{surf})$ to CO leads to quantitative conversion to $Ru_3(CO)_{12}$(ads), and the temperature dependence of the pseudo-first-order rate constants (Table II) yields an activation energy of 5.1 ± 0.4 kcal/mol. Comparing this value with that for reaction 1, 6.2 ± 0.4 kcal/mol, indicates that the grafted cluster, (μ-H)$Ru_3(CO)_{10}(\mu\text{-}OSi_{surf})$, is ca. 0.5 kcal/mol higher in energy than the physisorbed trimer, $Ru_3(CO)_{12}$(ads). The thermal reactions are reversible, and the interconversion between these energetically similar species can be considered a dynamic equilibrium where the extent of reaction is subject to factors which control the position of equilibrium. For example, the extent of reaction 1 is proportional to the volume of the photolysis cell. This is a consequence of the evolution of CO during the reaction. In a closed cell, the pressure rise due to evolved CO is largest in cells of small volume. As the pressure increases, the fraction of CO that desorbs decreases thereby increasing the probability of the back-reaction. Continuous removal of the CO, on the other hand, leads to quantitative conversion to the grafted cluster. Increasing the pressure of an inert gas also reduces the extent of reaction 1. The reason for this effect is not immediately apparent, but as suggested by a reviewer, the inert gas could compete for surface sites thereby diminishing the number of sites available to CO on its dissociation from the photogenerated intermediate.

The difference in the photoreactivity of the adsorbed complex, relative to that in fluid solution, does not appear to be due to the formation of a different primary photoproduct. The electronic spectrum of the adsorbed complex is within experimental error of that in fluid solution,[39] and as found for fragmentation in fluid solution,[22] reaction 1 is independent of excitation wavelength. We propose that the primary photoproduct generated on PVG is equivalent to that generated in fluid solution, i.e., an isomeric form of the trimer possessing a coordinatively unsaturated Ru center. Subsequent reactivity, however, reflects constraints imposed by the support.

Hydroxylated surfaces can be viewed as a polydentate ligand[65,66] where each surface functionality represents a potential two-electron donor. The reactivity of the primary photoproduct will therefore reflect the availability of these groups. Although dependent on previous heatings, studies of a variety of hydroxylated silicas indicate four to seven silanol groups/100 Å^2.[67,68] Taking 5 Å as the radius of $Ru_3(CO)_{12}$(ads), the planar surface area covered by the adsorbed trimer is 78 Å^2. Assuming that the primary photoproduct occupies essentially the same surface area, three to five silanol groups are in its immediate vicinity. Of course, the assumption that all silanol groups are equally reactive is suspect since, by the very nature of an amorphous material, not all are equivalent. Silanol groups have been differentiated by the extent of hydrogen bonding,[33,34,68,69] and DRIFT spectra of calcined PVG (see paragraph at end of paper regarding supplementary material) indicate the presence of both isolated and associated, i.e. hydrogen-bonded, silanol groups. In our opinion, the reactivity of the primary photoproduct toward different scavengers in solution suggests that it is sufficiently reactive to show little discrimination based on differences in H bonding. On the basis of three to five silanol groups in the immediate vicinity, the quantum yield of formation of (μ-H)$Ru_3(CO)_{10}(\mu\text{-}OSi_{surf})$, $(1.6 \pm 0.3) \times 10^{-2}$, is a reasonable approximation of the limiting yield. Therefore, relative to the limiting yield of fragmentation in fluid solution, $(7.4 \pm 3.0) \times 10^{-2}$, the smaller yield of the precursor complex on PVG is not due to a lack of available silanol groups. In view

(63) Nakamoto, K. *Infrared and Raman Spectra of Inorganic and Coordination Compounds*, 3rd ed.; Wiley-Interscience: New York, 1980; p 290.
(64) Johnson, B. F. G. *Transition Metal Clusters*; Johnson, B. F. G., Ed.; Wiley: New York, 1980; p 29.
(65) Burwell, R. L.; Pearson, R. G. *Inorg. Chem.* **1965**, *4*, 1123.
(66) Maatman, R. W. U.S. Atomic Energy Commission Report COO-1354-5; NTIS: Springfield, VA, 1965.
(67) Reference 32, pp 622–714.
(68) Snyder, L. R.; Ward, J. W. *J. Phys. Chem.* **1966**, *70*, 3941–52.
(69) Low, M. J. D.; Ramasubramanian, N. *J. Phys. Chem.* **1966**, *70*, 2740–6.

of the solvent dependence of the fragmentation yield,[22] the smaller yield found on PVG must reflect a more efficient nonradiative relaxation of the excited complex and/or a less efficient formation of the isomeric form possessing a coordinatively unsaturated metal center.

The calculated number of silanol groups must be regarded as an approximation, but a reaction controlled only by the silanol number would be expected to produce a mixture of monomeric and cluster reaction products. Since UV photolysis of $Ru_3(CO)_{12}$ physisorbed onto partially dehydroxylated silica (Carbosil) is reported to yield monomeric $Ru(CO)_4$–OSi_{surf} complexes,[24] in those regions where the density of silanol groups is sufficient, fragmentation to monomeric products would occur, whereas in regions of lower silanol number, oxidative addition of a single group may occur. The result would be a mixture of reaction products that is inconsistent with the observed specificity of reaction 1. In a sense, formation of the oxidative-addition product is similar to the steps leading to fragmentation in fluid solution. Yet, relative to fluid solution where fragmentation occurs with even less than a stoichiometric amount of a scavenger,[22] the absence of photofragmentation on PVG is not due to an inability to form the precursor complex or a lack of potential two-electron donors.

Wrighton and co-workers attribute the absence of a fragmentation pathway in the photochemistry of $Ru_3(CO)_9L_3$, where L represents a coordinated phosphine functionality anchored to silica gel, to constraints imposed by the functionalized support.[25] Since $Ru_3(CO)_{12}$ is physisorbed onto PVG, the constraints imposed on the complex arise from the support per se, rather than from a distinct chemical interaction. Turro has shown, in the case of dibenzyl ketones on zeolites, that the topology of the adsorbent surface affects photochemical reactivity.[30] In our opinion, it is the rigidity and topology[26-29,70] of the PVG surface, as opposed to the fluidity of a solvent cage, that limits the reaction to the oxidative addition of a single silanol group, and curtails the ability of the primary photoproduct to fragment to monomeric products. While rigidity and topology offer a rationale for the inability to model reaction 1 in fluid solution, it is not immediately apparent that they account for the differences in reactivity on Carbosil and PVG. Clearly, additional quantitative data on the photochemistry of molecules adsorbed onto chemically similar surfaces of characterized dimensionality are necessary to understand, and perhaps distinguish, the role of surface topology.

(70) Even, U.; Rademann, K.; Jortner, J.; Manor, N.; Reisfeld, R. *Phys. Rev. Lett.* **1984**, *52*, 2164-7.

Conclusion

UV photolysis of Ru_3CO_{12} physisorbed onto porous Vycor glass leads to oxidative addition of a surface silanol group and quantitative formation of (μ-H)Ru_3CO_{10}(μ-OSi_{surf}). Relative to fluid solution, the specificity of the reaction on PVG is a consequence of the rigidity and topology of the glass surface.

Acknowledgment. Support of this research by the Research Foundation of the City University of New York, the Dow Chemical Co. Technology Acquisition Program, and the National Science Foundation (Grant CHE-8511727) is gratefully acknowledged. H.D.G. thanks the Andrew W. Mellon Foundation for a fellowship during 1984, Queens College for a Presidential Research Award during 1987, and the Corning Glass Works for samples of porous Vycor glass.

Registry No. $Ru_3(CO)_{12}$, 15243-33-1; $Ru(CO)_4(PPh_3)$, 21192-23-4; $Ru(CO)_3(PPh_3)_2$, 14741-36-7; $Ru(CO)_4(P(t\text{-}Bu)_3)$, 69661-89-8; $Ru_3(CO)_{11}(PPh_3)$, 38686-52-1; PPh_3, 603-35-0; $P(t\text{-}Bu)_3$, 13716-12-6; CO, 630-08-0; 1-pentene, 109-67-1.

Supplementary Material Available: Figure 1S (infrared spectra recorded during 350-nm photolysis of a deaerated *n*-pentane solution containing 10^{-4} M $Ru_3(CO)_{12}$ and 10^{-3} M PPh_3), Figure 2S (dependencies of the quantum yield of declustrification on the concentration of PPh_3, 1-pentene, and $P(t\text{-}Bu)_3$), and Figure 3S (diffuse reflectance FTIR spectrum of PVG calcined at 550 °C) (3 pages). Ordering information is given on any current masthead page.

Contribution from the Department of Chemistry and Biochemistry, University of Colorado, Boulder, Colorado 80309

Synthesis and Reactivity of an Unusual Oxidation Product of $[C_5H_5Mo(\mu\text{-}S)(\mu\text{-}SH)]_2$

L. D. Tanner, R. C. Haltiwanger, J. Noordik, and M. Rakowski DuBois*

Received September 11, 1987

The reaction of a dilute solution of $[CpMo(\mu\text{-}S)(\mu\text{-}SH)]_2$ (Cp = C_5H_5) with 1 equiv of phenylacetylene under air leads to the formation of *anti*-$CpMo(O)(\mu\text{-}S)_2Mo(SCH{=}C(Ph)S)Cp$ (**1**) in 20% yield. Both syn and anti isomers of **1** can be synthesized by the reaction of $[CpMo(SCH{=}C(Ph)S)]_2$ with trifluoroacetic acid under air. The anti isomer has been characterized by an X-ray diffraction study. The complex crystallizes in space group $Pna2_1$, with a = 10.284 (6) Å, b = 15.175 (8) Å, c = 12.018 (7) Å, and V = 1875 (2) Å^3. The dinuclear complex contains two μ-sulfido ligands in a nonplanar Mo_2S_2 core, a terminal oxo ligand on one CpMo site, and a bidentate styrenedithiolate ligand coordinated to the second CpMo site. The cyclopentadienyl ligands are anti with respect to the metal–metal vector. The terminal oxo ligand in **1** is displaced by sulfide in the reaction with hexamethyldisilthiane. Complex **1** reacts with hydrogen to form water, $(CpMo)_2S_4$ derivatives, and organic products that result from hydrogenation and hydrolysis of the styrenedithiolate ligand.

Introduction

During the course of our studies of cyclopentadienylmolybdenum complexes with bridging sulfido ligands, we have reported that these systems react with alkynes to form complexes with alkenedithiolate ligands, e.g., eq 1.[1-3] Although $[CpMo(\mu\text{-}S)(\mu\text{-}SH)]_2$ is slightly air sensitive, reaction 1 generally proceeds to give the indicated products even in the presence of air. However, when the hydrosulfido complex was reacted with only 1 equiv of an alkyne in the presence of air, we isolated an additional unusual product that had added both an oxygen atom and an alkyne molecule to the $Cp_2Mo_2S_4$ core. In this paper we report the synthesis, spectroscopic characterization, and an X-ray diffraction study of one of these products of composition $Cp_2Mo_2S_4O$-

$$[CpMo(\mu\text{-}S)(\mu\text{-}SH)]_2 + \text{excess } RC{\equiv}CR \longrightarrow$$

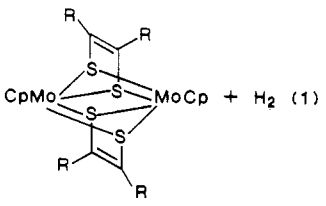

+ H_2 (1)

(1) Rakowski DuBois, M.; Haltiwanger, R. C.; Miller, D. J.; Glatzmaier, G. *J. Am. Chem. Soc.* **1979**, *101*, 5245.
(2) Rakowski DuBois, M.; Van Derveer, M. C.; DuBois, D. L.; Haltiwanger, R. C.; Miller, W. K. *J. Am. Chem. Soc.* **1980**, *102*, 7456.
(3) McKenna, M.; Wright, L. L.; Miller, D. J.; Tanner, L.; Haltiwanger, R. C.; Rakowski DuBois, M. *J. Am. Chem. Soc.* **1983**, *105*, 5329.

0020-1669/88/1327-1736$01.50/0